Applied Surface Science xxx (2017) xxx–xxx

Contents lists available at ScienceDirect

Applied Surface Science

journal homepage: www.elsevier.com/locate/apsusc

Optical response of gold hemispheroidal lattices on transparent substrates

Morten Kildemo[a,*], Jean-Philippe Banon[a], Alexandre Baron[b], Brage B. Svendsen[a], Thomas Brakstad[a], Ingve Simonsen[a,c]

[a] Department of Physics, NTNU Norwegian University of Science and Technology, NO-7491 Trondheim, Norway
[b] CNRS, Centre de Recherche Paul Pascal, UPR 8641 115 Avenue Schweitzer, 33600 Pessac, France
[c] Surface du Verre et Interfaces, UMR 125 CNRS/Saint-Gobain, F-93303 Aubervilliers, France

ARTICLE INFO

Article history:
Received 30 July 2016
Received in revised form 2 February 2017
Accepted 2 February 2017
Available online xxx

Keywords:
Mueller Matrix Ellipsometry
Plasmonics
Optical properties
Polarimetry

ABSTRACT

Square arrays of gold (Au) hemispheroids deposited on a UV-transparent glass substrate reveal a rich optical response when investigated by spectroscopic Mueller Matrix Ellipsometry. Two samples were studied; the first consisted of hemispheroids of parallel radius of 58 nm and height 30 nm with lattice constant 210 nm; the corresponding parameters for the second sample were 38 nm, 20 nm and 125 nm, respectively. By a full azimuthal rotation of the samples, we observe all the Rayleigh anomalies corresponding to grazing diffracted waves, with strong resonances for co-polarization scattered light near the high symmetry points and cross-polarization scattered light around the Localized Surface Plasmon Resonance. Polarization-conversion becomes particularly important at grazing incidence, and the cross-polarization follows the Rayleigh lines. The optical response (neglecting polarization conversion) is modelled in the quasi-static approximation using the so-called Bedeaux-Vlieger formalism, and the Finite Element Method using COMSOL. The direct inversion of the effective (substrate dependent) dielectric function is discussed.

1. Introduction

Mueller matrix ellipsometry is expected to play an important role in the characterization of plasmonic based devices, such as plasmonic metamaterials/metasurfaces [1,2], or composite nanoplasmonic devices with applications ranging from optoelectronics to biomedicine [3–5]. The fascinating properties of metamaterials can be exemplified by e.g. the negative refractive index [6] and its application to perfect lensing and subdiffraction imaging [7].

The metamaterials approach consists in determining effective electromagnetic parameters for an inhomogeneous periodic artificial material. As such, the metamaterials approach bridges the gap between low-frequency effective medium theory and the high frequency diffractive regime (therein photonic crystals) [8]. However, it is necessarily the combined response that will be observed by spectroscopy across a larger spectral range.

Here we study an apparently simple model system consisting of hemispheroidal Au particles organized in a square lattice on a UV-transparent flat glass substrate. The particle dimensions are such that the quasistatic approximation should be valid, at least for the longest wavelengths. This system was recently shown to have a rich optical response including polarization coupling around the Localized Surface Plasmon Resonance (LSPR), and around so-called Rayleigh anomalies (or Rayleigh lines) related to grazing diffracted waves just at the onset of diffracted orders [2].

Indeed, the importance of the polarization coupling can be directly observed in Mueller matrix spectroscopic studies with complete azimuthal sample rotation of inherently anisotropic systems, such as self-assembled Ag or Au particles along the ripples of a nanopatterned substrate [9–11], meta-surfaces of U-shaped particles [12], slanted metallic pillars [13], and chiral structures [14].

In this paper, the regular lattices of idealized metallic hemispheroids supported by a flat dielectric substrate (here SiO_2) are modelled by the Bedeaux-Vlieger theory [15]. Since this theory does not account for cross-polarized scattered light, only a block-diagonal Mueller matrix can be obtained within this approach. In order to account for cross-polarized scattered light, and therefore obtaining non-vanishing off-diagonal elements of the Mueller matrix, more accurate and time consuming modelling approaches have to be used. One possibility is to perform the modelling on

* Corresponding author.
E-mail address: Morten.Kildemo@ntnu.no (M. Kildemo).

http://dx.doi.org/10.1016/j.apsusc.2017.02.008
0169-4332/

the basis of the reduced Rayleigh equation [16,17] which recently was shown to produce reliable results for the Mueller matrix elements [18]. Other approaches, often used in the metamaterials community, are the full wave solutions obtained by the Finite Element Method (FEM) and Finite Difference Time Domain (FDTD) simulations. In this work we will present results obtained by FEM simulations.

2. Experimental

The samples were produced by evaporating a thin film of Au onto a clean (and flat) UV-grade fused silica surface using an e-beam evaporator (Pfeiffer Vacuum Classic 500). The deposited film thicknesses were 40 nm (Sample A) and 20 nm (Sample B). The resulting films were smooth but polycrystalline. The Au nano-structures on glass were produced by Focused Ion Beam (FIB)-milling using Ga ions (FEI Helios Dual-beam FIB). The two samples reported here were manufactured to make up Au hemispheroids distributed in a square pattern on a glass-surface, see Fig. 1(a); the lattice constants were $a = 210\,nm$ (Sample A) and $a = 125\,nm$ (Sample B). After the milling, the particles were found to be hemispheroids of lateral radius $R_{xy} = (58 \pm 4)$ nm (Sample A), and (38 ± 4) nm (Sample B), see Fig. 1(c). The heights of the particles (the perpendicular radii) were difficult to estimate accurately from the combination of AFM and SEM images. However, rough estimates are $R_z = 30\,nm$ for Sample A (<40 nm) and $R_z = 25\,nm$ for Sample B (with an expected uncertainty of several nanometers). Unfortunately, an over-etching into the substrate was observed for both samples, i.e. the Au particles are probably on top of a dielectric mound, as roughly sketched in Fig. 1(d). Both samples had an over-milling of at least 10 nm into the substrate.

The surface coverage for a square lattice of hemispheroidal particles is defined as $\Theta = \pi R_{xy}^2/a^2$, giving $\Theta_A = 0.20$ and $\Theta_B = 0.18$ for the coverage of Sample A and Sample B, respectively.

For the optical characterization of the samples, a variable angle multichannel dual rotating compensator Mueller matrix ellipsometer (RC2) from JA Woollam Company was used. Our instrument has a collimated 150 W Xe source and operates in the spectral range from 210 nm (5.9 eV) to 1700 nm (0.73 eV). As the FIB-milling is a time consuming process, the total milling area opened by FIB was limited to 240 μm × 240 μm. Focusing and collection lenses with a focal length of 20 mm and a Numerical Aperture of approximately 0.15, were applied, allowing a normal incidence spot size of smaller 100 μm. This spot size allowed us to study the full azimuthal rotation of the sample while ensuring that the spot-size remained within the 240 μm × 240 μm area. The spectroscopic Mueller matrix was measured for the polar incidence angles (with respect to surface normal) $\theta_0 = 45°$, 55° and 65°. Full azimuthal rotation of the sample around the sample normal (360°) in steps of 5° was performed for each polar angle of incidence in order to fully map any anisotropy in the optical response of the sample (see Brakstad et al. [2] for further details).

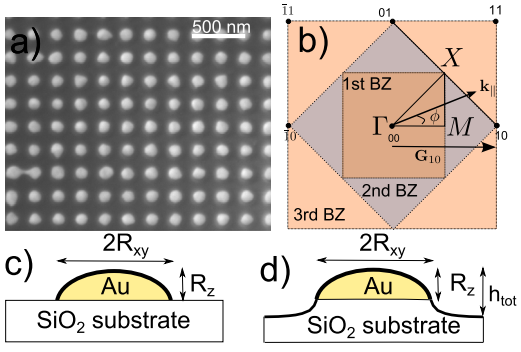

Fig. 1. (a) Real space Scanning Electron Microscopy (SEM) image of the particle array. (b) Schematic drawing of the 2-dimensional reciprocal lattice defining ϕ_0. (c) The ideal model consisting of a hemispheroidal Au particle on uv-transparent glass. (d) The presumed non-ideal model with the particles on a mound.

3. Results and discussion

3.1. Mueller matrix: LSPR, Rayleigh lines and polarization coupling

Fig. 2 presents an overview of the normalized Mueller matrix optical response, **m**, measured for Sample A as a function of the photon energy ($E = \hbar\omega$), for the specular direction $[(\theta_0, \phi_0) = (\theta_s, \phi_s)]$. A series of measurements were performed for a fixed polar angle of incidence $\theta_0 = 55°$, but different values of the azimuthal angle of incidence ϕ_0. The coordinate system is defined so that the value $\phi_0 = 0°$ represents a direction that coincides with one of the main axes of the square lattice. In Fig. 2 the (2×2) block diagonal elements of **m** are stacked as functions of the azimuthal angle of incidence (except m_{22}). The corresponding SEM image of Sample A and a schematic diagram of the reciprocal lattice are shown in Fig. 1(a) and (b), respectively, see also Figs. 1–3 in Brakstad et al. [2]. We observe from the diagonal elements of the Mueller matrix that a LSPR exists for a photon energy around 2.1 eV, which is here found to be slightly dispersive with azimuthal rotation angle ϕ_0, see also Ψ_{pp} and $\langle\varepsilon\rangle_{pp}$ in Ref. [2]. Furthermore, we observe polarization conversion around the LSPR that dependends on ϕ_0; this is seen from the off-block-diagonal elements (which are not stacked) in Fig. 2. We further observe that there are prominent features in both the block-diagonal elements (dips and peaks) and the off-block-diagonal elements (strong polarization conversion); these features are attributed to the Rayleigh anomalies [19] as previously described in detail in Brakstad et al. [2] and references therein.

In recent works [2,9,20,21] we have found it useful to present Mueller matrix data in terms of contour plots in polar coordinates as they clearly show their dependence on the rotation of the sample. In such plots, the polar coordinate corresponds to the azimuthal rotation angle (ϕ_0) and the radial coordinate represents the photon energy. Fig. 3 presents in this fashion the normalized Mueller matrix data of which the data-sets from Fig. 2 are subsets; the inner and outer circles in Fig. 3 correspond to 0.73 eV and 5.9 eV, respectively. Notice that for given azimuthal rotation angle (ϕ_0), a cut along the radial direction of the data-sets presented in Fig. 3 will result in curves for the same value of ϕ_0 that are similar to those in Fig. 2. Moreover, the data in Fig. 3 are organized such that $\phi_0 = \angle(\mathbf{k}_\parallel, \mathbf{G}_\parallel^{(10)})$, where the component of the incident wave vector parallel to the surface of the substrate is ($|\mathbf{k}| = k = n_0\omega/c$)

$$\mathbf{k}_\parallel = k \sin\theta_0(\cos\phi_0, \sin\phi_0, 0), \tag{1}$$

and the reciprocal lattice vector is defined as

$$\mathbf{G}_\parallel^{(\mathbf{l})} = l_1\mathbf{b_1} + l_2\mathbf{b_2} = G_\parallel^{(\mathbf{l})}(\cos\phi_{\mathbf{l}}, \sin\phi_{\mathbf{l}}, 0), \tag{2}$$

where l_1 and l_2 are integers and $G_\parallel^{(\mathbf{l})} = |\mathbf{G}_\parallel^{(\mathbf{l})}|$. In writing Eq. (2) we have introduced the primitive translation vectors of the reciprocal lattice $\mathbf{b}_1$ and $\mathbf{b}_2$ ($|\mathbf{b}_{1,2}| = 2\pi/a$), and defined the vector $\mathbf{l} = (l_1, l_2)$ (see Ref. [2] for further details).

It is observed from Fig. 3 that the Mueller matrix of Sample A is nearly block-diagonal for photon energies up till about 3 eV, and the same was found also for Sample B (results not shown). The LSPR is now observed as the nearly circular features around 2.1 eV in all the block diagonal elements presented in Fig. 3. The Rayleigh lines observed in e.g. the m_{12} element, now make up a set of features that resembles the first and second Brillouin zone (BZ), see Fig. 1(b).

Brakstad et al. [2] described thoroughly the main features of these Rayleigh lines [19]. In particular, in this work, a compact

Please cite this article in press as: M. Kildemo, et al., Optical response of gold hemispheroidal lattices on transparent substrates, Appl. Surf. Sci. (2017), http://dx.doi.org/10.1016/j.apsusc.2017.02.008